FLUX BALANCE AND SELF-SIMILAR LAWS OF WIND WAVE GROWTH

S. I. Badulin[(1)], A. V. Babanin[(2)], A. N. Pushkarev[(3)], V. E. Zakharov[(3,4,5)], D. T. Resio[(6)]

[(1)] P.P.Shirshov Institute of Oceanology (bsi@wave.sio.rssi.ru/Fax: [7] 095 124 59 83), Russia
[(2)] Swinburne University of Technology, Melbourne, Australia
[(3)] Landau Institute for Theoretical Physics, Russia
[(4)] University of Arizona, USA
[(5)] Waves and Solitons, LLC, USA
[(6)] Waterways Experimental Station,USA

1. INTRODUCTION. THE SPLIT BALANCE MODEL OF WIND-DRIVEN SEAS

The Hasselmann equation (Hasselmann 1962, Hasselmann 1963)

$$\frac{\partial N_{\mathbf{k}}}{\partial t} + \nabla_{\mathbf{k}}\omega_{\mathbf{k}}\nabla_{\mathbf{r}}N_{\mathbf{k}} = S_{nl} + S_f \tag{1}$$

is a core of all the modern wind-wave prediction models. It describes evolution of wave action spectral density $N(\mathbf{k}, t)$ due to four-wave nonlinear resonant interactions (the so-called collision integral S_{nl}) and external forcing S_f. The fundamental solutions of the conservative Hasselmann equation have been found in the sixties (Zakharov & Filonenko 1966, Zakharov 1966, Zakharov & Zaslavskii 1982). These solutions represent remarkable examples of the so-called flux solutions that provide constant fluxes of the first integrals: energy, action and momentum from infinitely small or large scales to opposite infinity. Energy and momentum are conserved formally only within the Hasselmann equation: they can leak to high frequency. Thus, the equation is not "complete", describe an "open system" and, in this sense, is not physically correct. The external input S_f appears to be of key importance for the Hasselmann equation and makes the Hasselmann equation both physically and mathematically correct. This is in contrast with the classic Boltzmann equation for ideal gas dynamics which solutions are unique at any initial data and conserve action, energy and momentum.

A correct account of external forcing is not a trivial problem for the case of wind-driven waves: the wave growth and dissipation are governed by multiple physical mechanisms which mathematical and physical description is not well elaborated yet. Experimental parameterizations of S_f by different authors give dispersion of magnitudes that exceeds the magnitude of S_f itself (see Hsiao & Shemdin 1983, Plant 1982, Snyder et al. 1981, Stewart 1974, Donelan & Pierson-jr. 1987). The basic feature of wind-wave dynamics can help to resolve the difficulty of description of external forcing: in a wide range of physical conditions the nonlinear transfer term S_{nl} dominates over external forcing term S_f. Thus, an asymptotic method can be developed for the Hasselmann equation (1). The procedure "split" the wind-wave balance into two parts: spectra are described by conservative Hasselmann equation

$$\frac{\partial N_{\mathbf{k}}}{\partial t} + \nabla_{\mathbf{k}}\omega_{\mathbf{k}}\nabla_{\mathbf{r}}N_{\mathbf{k}} = S_{nl} \tag{2}$$

while external forcing gives a boundary condition for quantities averaged over the whole angle-frequency space (Badulin et al. 2002, Pushkarev, Resio & Zakharov 2003, Badulin et al. 2005)

$$\langle\frac{\partial N_{\mathbf{k}}}{\partial t} + \nabla_{\mathbf{k}}\omega_{\mathbf{k}}\nabla_{\mathbf{r}}N_{\mathbf{k}}\rangle = \langle S_f\rangle \tag{3}$$

A family of self-similar solutions of the system (2,3) can be considered as a generalization of the Kolmogorov-Zakharov solutions (Badulin et al. 2005). These solutions provide cascades of wave action, energy and momentum that depend both on frequency and time (fetch). The feature of the solutions is in rigid link of the solutions themselves with the spectral fluxes quite similar to the classic Kolmogorov-Zakharov solutions (Zakharov & Filonenko 1966, Zakharov & Zaslavskii 1982).

The validity of the split balance model (2,3) in terms of self-similarity features of the solutions of the full Hasselmann equation has been demonstrated in our previous papers (Badulin et al. 2002, Badulin

et al. 2005). In the present paper we show that solutions of the Hasselmann equation as well as the corresponding spectral fluxes have certain features of quasi-universality. This fact allows us to formulate an asymptotic growth law of wind-driven waves that relates total wave energy (the same is valid for wave action and momentum) with the corresponding spectral flux at infinitely high frequency. The latter characteristic can be associated with the total wave input.

In the present paper we focus on the case of the homogeneous Hasselmann equation

$$\frac{\partial N(\mathbf{k},t)}{\partial t} = S_{nl} + S_f \tag{4}$$

Similar results can be formulated for the stationary counterpart (the so-called fetch-limited case)

$$\frac{\partial \omega}{\partial k}\frac{\partial N(\mathbf{k},t)}{\partial x} = S_{nl} + S_f \tag{5}$$

In § 2 we give definitions and general relationships for self-similar solutions and the corresponding spectral fluxes for the case of duration-limited growth (4). In § 3 we present numerical results that illustrate quasi-universality of the solutions and fluxes and allows us to formulate the asymptotic wave growth law. This growth law contains a parameter — an analogue of the classic Kolmogorov constants that should be found numerically. In § 4 we cosider sea wave experiments that justify our theoretical findings. In § 5 we discuss Toba's law as a particular case of wind-wave growth and recent experimental study (Resio, Long & Vincent 2004) which use very close approach to the analysis of balance of wind-driven waves. § 6 gives a summary of the study.

2. SELF-SIMILAR SOLUTIONS OF THE HASSELMANN EQUATION AS A GENERALIZATION OF THE KOLMOGOROV-ZAKHAROV SOLUTIONS

2.1 Self-similar solutions for duration-limited case

The split balance model (2,3) admits a two-parametric family of self-similar solutions for duration-limited case

$$\begin{aligned} N = a_\tau t^{\alpha_\tau}\Phi_{\beta_\tau}(\boldsymbol{\xi}); \qquad \boldsymbol{\xi} &= b_\tau \mathbf{k} t^{\beta_\tau} \\ \alpha_\tau &= (19\beta_\tau - 2)/4; \\ b_\tau &= a_\tau^{4/19} \end{aligned} \tag{6}$$

The relationship between exponents of spectral growth α_τ and downshift β_τ and between magnitude of spectrum a_τ and spectral width b_τ are fixed by homogeneity property of collision integral only.

The "shape" function $\Phi_{\beta_\tau}(\boldsymbol{\xi})$ is to be determined from an integro-differential equation

$$\begin{aligned} \left[\alpha_\tau\Phi_{\beta_\tau} + \beta_\tau\boldsymbol{\xi}\nabla_{\boldsymbol{\xi}}\Phi_{\beta_\tau}\right] &= \pi\int \mathrm{d}\boldsymbol{\xi}_1\mathrm{d}\boldsymbol{\xi}_2\mathrm{d}\boldsymbol{\xi}_3 |T_{\boldsymbol{\xi}\boldsymbol{\xi}_1\boldsymbol{\xi}_2\boldsymbol{\xi}_3}|^2 \\ &\times \delta(\boldsymbol{\xi}+\boldsymbol{\xi}_1-\boldsymbol{\xi}_2-\boldsymbol{\xi}_3)\delta(\sqrt{|\boldsymbol{\xi}|}+\sqrt{|\boldsymbol{\xi}_1|}-\sqrt{|\boldsymbol{\xi}_2|}-\sqrt{|\boldsymbol{\xi}_3|}) \\ &\times [\Phi_{\beta_\tau}(\boldsymbol{\xi}_1)\Phi_{\beta_\tau}(\boldsymbol{\xi}_2)\Phi_{\beta_\tau}(\boldsymbol{\xi}_3) + \Phi_{\beta_\tau}(\boldsymbol{\xi})\Phi_{\beta_\tau}(\boldsymbol{\xi}_2)\Phi_{\beta_\tau}(\boldsymbol{\xi}_3) \\ &- \Phi_{\beta_\tau}(\boldsymbol{\xi})\Phi_{\beta_\tau}(\boldsymbol{\xi}_1)\Phi_{\beta_\tau}(\boldsymbol{\xi}_2) - \Phi_{\beta_\tau}(\boldsymbol{\xi})\Phi_{\beta_\tau}(\boldsymbol{\xi}_1)\Phi_{\beta_\tau}(\boldsymbol{\xi}_3)] \end{aligned} \tag{7}$$

We assume that physically relevant solutions of (7) exist and focus upon higher order approximation of the evolution problem. The form of solutions (6) provides a power-like growth of total wave action (or energy). The balance equation (3) can be satisfied trivially

$$\int N(\mathbf{k})\mathrm{d}\mathbf{k} = a^{11/19}t^{r_\tau}\int \Phi_{\beta_\tau}(\boldsymbol{\xi})\mathrm{d}\boldsymbol{\xi} \tag{8}$$

Integration in (8) implies the whole wavevector space. For total wave energy one has

$$\varepsilon = \int \omega(\mathbf{k})N(\mathbf{k})\mathrm{d}\mathbf{k} = a_\tau^{9/19}g^{1/2}t^{p_\tau}\int |\boldsymbol{\xi}|^{1/2}\Phi_{\beta_\tau}(\boldsymbol{\xi})\mathrm{d}\boldsymbol{\xi} \tag{9}$$

and mean frequency evolves as follows

$$\omega_m = \frac{\int \omega(\mathbf{k})\varepsilon(\mathbf{k})\mathrm{d}\mathbf{k}}{\varepsilon} = a_\tau^{-2/19} g^{1/2} t^{-q_\tau} \frac{\int |\boldsymbol{\xi}| \Phi_{\beta_\tau}(\boldsymbol{\xi})\mathrm{d}\boldsymbol{\xi}}{\int |\boldsymbol{\xi}|^{1/2} \Phi_{\beta_\tau}(\boldsymbol{\xi})\mathrm{d}\boldsymbol{\xi}} \tag{10}$$

Assuming

$$\max(\Phi_{\beta_\tau}) = \Phi_{\beta_\tau}(1) \tag{11}$$

one can define peak frequency

$$\omega_p = a_\tau^{-2/19} g^{1/2} t^{-q_\tau} \tag{12}$$

Mean frequency ω_m and the peak one ω_p are proportional to each other for the self-similar solutions (6) as it is seen from (10,12). Exponents of spectral growth p_τ, r_τ and frequency downshift q_τ appear to be linked to each other by simple linear relations

$$\begin{aligned} r_\tau &= \alpha_\tau - 2\beta_\tau \\ p_\tau &= \alpha_\tau - 5\beta_\tau/2 \\ q_\tau &= \beta_\tau/2 \end{aligned} \tag{13}$$

The self-similar solutions (6) predict power-law dependencies (9,10,12) quite similar to experimental dependences of wind-wave growth (see e.g. Davidan et al. 1995, Babanin & Soloviev 1998). A key feature of theoretical exponents is the linear dependence of exponent of total wave energy growth p_τ on downshift exponent q_τ

$$p_\tau = \frac{9q_\tau - 1}{2} \tag{14}$$

while in experimental dependencies this linkage of exponents p_τ and q_τ is not assumed.

Note, that validity of the asymptotic split balance model is difficult to check analytically. A trivial estimate can be derived from the condition that nonlinear transfer term should dominate at large time over wave input and dissipation which linear increments are finite (see Badulin et al. 2005, sect. 5.2 for details). It gives rough estimates

$$p_\tau > 4/19; \qquad q_\tau > 3/19 \tag{15}$$

i.e. the total wave input can decay with time but not too fast.

2.2 Self-similarity of spectral fluxes

Spectral fluxes of wave action, energy and momentum can be introduced in a standard way (see Zakharov & Pushkarev 1999, Zakharov 2005a)

$$Q(\omega) = \int_{\omega_l}^{\omega} \int_{-\pi}^{\pi} \frac{2\omega^3}{g^2} S_{nl}(\mathbf{k})\mathrm{d}\omega\mathrm{d}\theta \tag{16}$$

$$P(\omega) = -\int_{\omega_l}^{\omega} \int_{-\pi}^{\pi} \frac{2\omega^4}{g^2} S_{nl}(\mathbf{k})\mathrm{d}\omega\mathrm{d}\theta \tag{17}$$

$$K_x(\omega) = -\int_{\omega_l}^{\omega} \int_{-\pi}^{\pi} \frac{2\omega^5}{g^3} S_{nl}(\mathbf{k}) \cos\theta \mathrm{d}\omega\mathrm{d}\theta \tag{18}$$

Self-similarity of the solutions of the kinetic equation means, evidently, self-similarity of spectral fluxes. It allows one to obtain remarkable expressions for the spectral fluxes in terms of shape functions $PHI_\beta(\boldsymbol{\xi})$

$$\begin{aligned}
\frac{Q(\omega,t)}{a^{11/19}g^{3/2}t^{s_q}} &= Q_\beta(\boldsymbol{\xi}) = \int\limits_{-\pi}^{\pi}\int\limits_{0}^{|\boldsymbol{\xi}|}(\beta|\boldsymbol{\xi}|^2\frac{\partial\Phi_\beta}{\partial|\boldsymbol{\xi}|}+\alpha|\boldsymbol{\xi}|\Phi_\beta)\mathrm{d}|\boldsymbol{\xi}|\mathrm{d}\theta \\
&= \left[\int\limits_{-\pi}^{\pi}\beta|\boldsymbol{\xi}|^2\Phi_\beta\mathrm{d}\theta\Big|_0^{|\boldsymbol{\xi}|} + r_\tau\int\limits_{-\pi}^{\pi}\int\limits_{0}^{|\boldsymbol{\xi}|}|\boldsymbol{\xi}|\Phi_\beta\mathrm{d}|\boldsymbol{\xi}|\mathrm{d}\theta\right] \qquad (19)\\
\frac{P(\omega,t)}{a^{9/19}g^{2}t^{s_p}} &= P_\beta(\boldsymbol{\xi}) = -\int\limits_{-\pi}^{\pi}\int\limits_{0}^{|\boldsymbol{\xi}|}(\beta|\boldsymbol{\xi}|^{5/2}\frac{\partial\Phi_\beta}{\partial|\boldsymbol{\xi}|}+\alpha|\boldsymbol{\xi}|^{3/2}\Phi_\beta)\mathrm{d}|\boldsymbol{\xi}|\mathrm{d}\theta = \\
&- \left[\int\limits_{-\pi}^{\pi}\beta|\boldsymbol{\xi}|^{5/2}\Phi_\beta(\boldsymbol{\xi})\mathrm{d}\theta\Big|_0^{|\boldsymbol{\xi}|} + p_\tau\int\limits_{-\pi}^{\pi}\int\limits_{0}^{|\boldsymbol{\xi}|}|\boldsymbol{\xi}|^{3/2}\Phi_\beta\mathrm{d}|\boldsymbol{\xi}|\mathrm{d}\theta\right] \qquad (20)\\
\frac{K(\omega,t)}{a^{7/19}g^{3/2}t^{s_m}} &= K_\beta(\boldsymbol{\xi}) = -\int\limits_{-\pi}^{\pi}\int\limits_{0}^{|\boldsymbol{\xi}|}(\beta|\boldsymbol{\xi}|^{3}\frac{\partial\Phi_\beta}{\partial|\boldsymbol{\xi}|}+\alpha|\boldsymbol{\xi}|^{2}\Phi_\beta)\mathrm{d}|\boldsymbol{\xi}|\mathrm{d}\theta = \\
&- \left[\int\limits_{-\pi}^{\pi}\beta|\boldsymbol{\xi}|^{3}\Phi_\beta(\boldsymbol{\xi})\mathrm{d}\theta\Big|_0^{|\boldsymbol{\xi}|} + m_\tau\int\limits_{-\pi}^{\pi}\int\limits_{0}^{|\boldsymbol{\xi}|}|\boldsymbol{\xi}|^{2}\Phi_\beta\mathrm{d}|\boldsymbol{\xi}|\mathrm{d}\theta\right] \qquad (21)
\end{aligned}$$

The result of the integration is of fundamental interest: for positive exponents of wave action growth r_τ and energy growth p_τ the signs of fluxes Q and P are fixed and correspond to inverse cascade regime, i.e. $Q > 0$, $P < 0$. The momentum flux is negative (inverse cascade) as well for rates $r_\tau > 2/7$ ($p_\tau > 1/7$). Note, that the small rates $r_\tau < 7/19$ are of little interest for our analysis because the smallness of source terms is questionable in this case (see Badulin et al. 2005). The case of swell is of special interest. The parameter p_τ is negative and both types of cascades are co-existing for wave energy and momentum: inverse cascade in a low frequency band (small $|\boldsymbol{\xi}|$) and a leakage of energy and momentum (direct cascade) in high frequencies.

2.3 Spectra vs spectral fluxes

Having self-similar dependencies for solutions (6) and fluxes (19) one can construct easily time-independent quantities which are direct analogues of the classic Kolmogorov's constants (Zakharov 1966, Zakharov 1999). In terms of frequency spectra it takes

$$C_q^{(\beta)}(\boldsymbol{\xi}) = \frac{E(\omega,\theta,t)\omega^{11/3}g^{4/3}}{Q(\omega,t)^{1/3}} = \frac{\Phi_\beta(\boldsymbol{\xi})|\boldsymbol{\xi}|^{11/3}}{Q_\beta(\boldsymbol{\xi})^{1/3}} \qquad (22)$$

$$C_p^{(\beta)}(\boldsymbol{\xi}) = \frac{E(\omega,\theta,t)\omega^{4}g^{4/3}}{P(\omega,t)^{1/3}} = \frac{\Phi_\beta(\boldsymbol{\xi})|\boldsymbol{\xi}|^{4}}{P_\beta(\boldsymbol{\xi})^{1/3}} \qquad (23)$$

$$C_m^{(\beta)}(\boldsymbol{\xi}) = \frac{E(\omega,\theta,t)\omega^{13/3}g^{4/3}}{K(\omega,t)^{1/3}} = \frac{\Phi_\beta(\boldsymbol{\xi})\boldsymbol{\xi}^{25/6}}{K_\beta(\boldsymbol{\xi})^{1/3}} \qquad (24)$$

The values $C_p(\boldsymbol{\xi})$, $C_q(\boldsymbol{\xi})$, $C_m(\boldsymbol{\xi})$ are direct generalizations of the Kolmogorov constants (see Zakharov & Filonenko 1966, Zakharov & Zaslavskii 1982, Zakharov 2005b). They depend on the self-similarity index r (or β) and on self-similarity argument $\boldsymbol{\xi}$ which is proportional to non-dimensional wavenumber (or wave frequency).

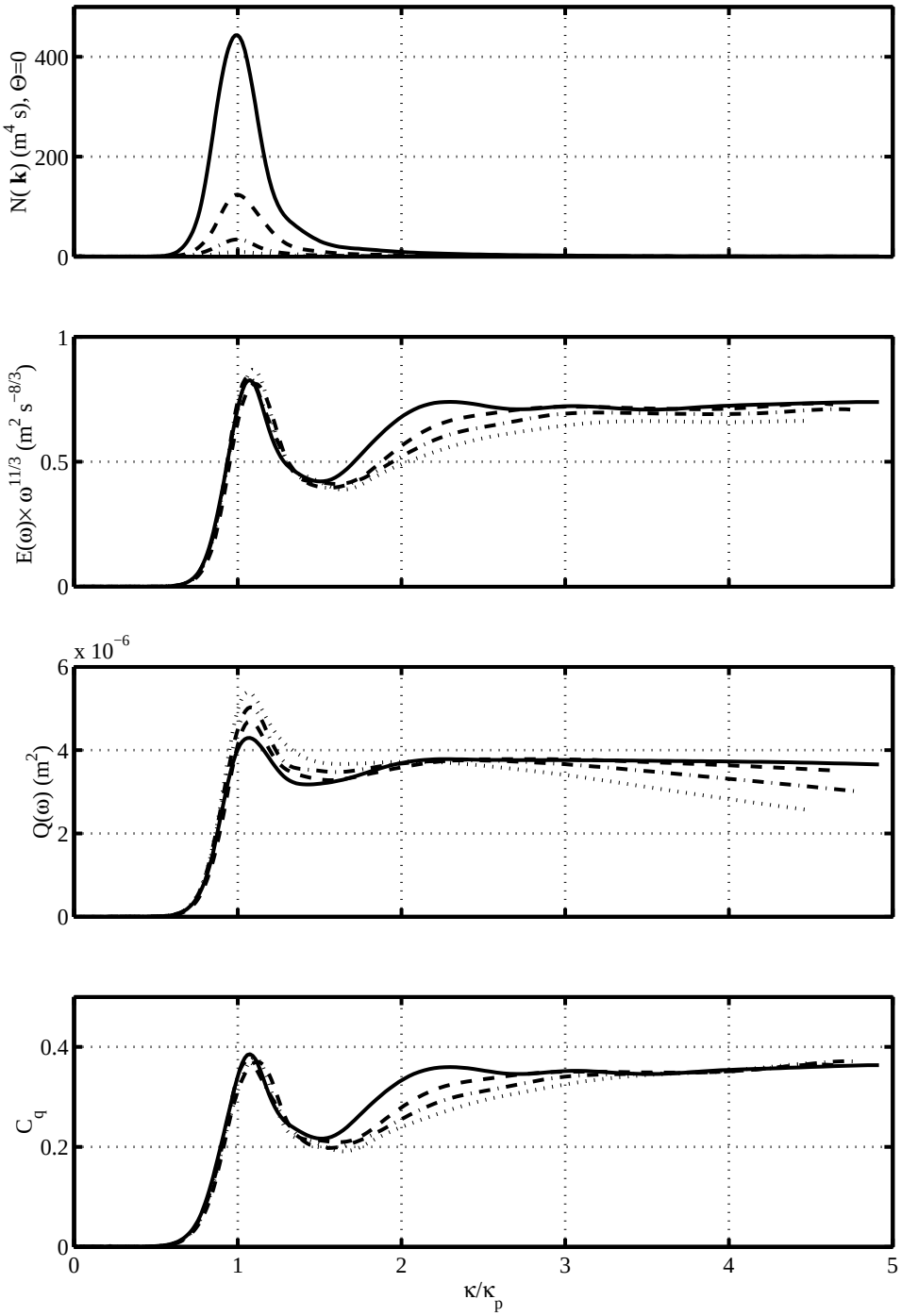

Figure 1: Down-wind solution $N(\mathbf{k})$, compensated frequency spectra of energy $E(\omega)\omega^{11/3}$, wave action flux Q and the resulting estimate of the Kolmogorov ratio C_q for solutions of the Hasselmann equation (1) at different times. Wave input (Hsiao & Shemdin 1983), wind speed 10 m·s^{-1}, time 4 (dotted), 8 (dash-dot), 16 (dashed), 32 hours (hard line)

Fig. 1 illustrates the asymptotic property of numerical solutions of the full Hasselmann equation (1) with the wave input (Hsiao & Shemdin 1983). The most rapid tendency to the asymptotic state is observed for the vicinity of spectral peak where nonlinear transfer has maximal magnitudes and, thus, perturbation to the model of split balance (2,3) dealing with smearing of wave input in wave scales is minimal. Similar strong tendency to an asymptotic state is seen for high frequencies where strong relaxation to weakly turbulent quasi-stationary asymptotics given by classic Zakharov-Kolmogorov cascade solutions (Zakharov & Filonenko 1966, Zakharov & Zaslavskii 1982) occurs due to high magnitudes of kernels of nonlinear interactions. The most pronounced deviations from the asymptotic behavior are seen in an intermediate wave range for the compensated spectra. This was explained in (Badulin et al. 2005) as an effect of a non-self-similar background in wave spectra. Wave action spectral fluxes appear to be not so sensitive to the background.

The self-similarity of solutions and fluxes makes possible alternative formulations of the basic physical feature of the problem: rigid link of wave spectra and spectral fluxes. The "boundary" condition of the split balance model (3) uses an integral wave input $\langle S_f \rangle$, i.e. a spectral flux at infinitely high frequencies ($|\boldsymbol{\xi}| = \omega/\omega_p \to \infty$) which is a power-law function of time (8,9). The characteristic frequency of the wave spectra, mean or peak frequency of the spectral shape, is also a power-law function. Accepting the split balance model it is logical to use these two values, total wave input and characteristic wave frequency, to use self-similarity of the problem "in full": to exclude an explicit dependence of the solutions (6) on time. Thus, after trivial algebra one gets for energy spectra corresponding to the self-similar solutions (6)

$$\frac{\varepsilon(\omega,\theta)\omega_*^5}{g^2} = \alpha_{ss}^* \left(\frac{\omega_*^3 \langle \mathrm{d}\varepsilon/\mathrm{d}t \rangle}{g^2} \right)^{1/3} \Phi_\beta(\omega/\omega_*, \theta) \tag{25}$$

Expression (25) has a typical form of the second type or incomplete self-similarity: there is a non-trivial dependence on one self-similar argument, non-dimensional frequency ω/ω_*, — the shape function Φ_β and a monotonic dependence on the second argument, non-dimensional integral wave input $\omega_*^3 \langle \mathrm{d}\varepsilon/\mathrm{d}t \rangle / g^2$. Both arguments represent the characteristic scales of the split balance model (2,3). Note the resemblance of the theoretical form (25) and conventional parameterizations of wind-wave spectra (see e.g. Hasselmann et al. 1973) which are, in fact, have the same second-type self-similarity form

$$\frac{\varepsilon(\omega,\theta)\omega_p^5}{g^2} = \alpha_{exp} (C_p/U_h)^{\kappa_\alpha} \Phi_{exp}(\omega/\omega_p, \theta, \gamma, \sigma_a, \sigma_b, \ldots) \tag{26}$$

The key difference of the theoretical and experimental results is in inner scaling: in the split balance model we follow here the scale is a total wave input, in experimental parameterizations the spectral magnitude is scaled by a characteristic wind speed (U_h — wind speed at a reference height or u^* — tension velocity of the atmospheric boundary layer). The wind scaling implies an incorporation of atmospheric dynamics into the model of wind-wave growth while the proposed split balance model split, in fact, the wind over waves dynamics and an inherent dynamics of weakly nonlinear waves. The difference in physics is illustrated by an additional arguments $\gamma, \sigma_a, \sigma_b, \ldots$, i.e. by dependence of spectral shapes Φ_{exp} on features of sea state: wave age, wind variability (Abdalla & Cavaleri 2002) *etc.* In our theoretical formulation the shape function Φ_β is determined by wave growth rate r_τ only.

The self-similarity solutions (25) can be re-written for total energy as well

$$\frac{\varepsilon\omega_*^4}{g^2} = \alpha_{ss} \left(\frac{\omega_*^3 \mathrm{d}\varepsilon/\mathrm{d}t}{g^2} \right)^{1/3} \tag{27}$$

Angle brackets are omitted here for total energy and input. Stress again, that in the weakly turbulent form (27) the parameter α_{ss} is not constant: it can depend on the index of self-similarity p_τ because of dependence of "shape function" Φ_β on p_τ. The spectral shapes are quasi-universal in duration-limited case (Badulin et al. 2002, Badulin et al. 2005) and, very likely, in fetch-limited case as well. Thus, one can expect a weak dependence of the self-similarity parameter α_{ss} on exponents of spectral growth. It makes the relation (27) useful for experimental verification.

Weak dependence of "shape function" Φ_β and parameter α_{ss} on self-similarity index p_τ (p_χ) has another important consequence: the self-similarity laws (25,27), very likely, work well not in a particular

case of power-like dependence of total flux on time (fetch) only but in general case of arbitrary time-(fetch-) dependence of total net forcing $\mathrm{d}\varepsilon/\mathrm{d}t$. This note just reflects our intuitive vision of the problem: self-similar solutions, as a rule, correspond to rather robust physical regimes and the features of the solutions can be observed at rather general physical conditions. In this sense we should emphasize once more weakly turbulent nature of the laws (25, 27) rather than their links with particular self-similar solutions of a set of equations (2,3).

3. NUMERICAL VERIFICATION OF WIND-WAVE GROWTH LAW

To check validity of the weakly turbulent laws (25,27) we start with duration-limited case. This case is extremely "inconvenient" for field studies and the list of representative experiments is rather short. This bad luck will be made up by results of extensive numerical study (Badulin et al. 2005). Time series of the numerical experiments allow one to validate the weakly turbulent dependences, first of all, in terms of relationships for self-similar solutions (14, 27) by simple fitting the series by power-like dependences. This somewhat restrictive approach can be avoided as far as we appreciate the fact of the weakly turbulent relationship of energy and flux (25) that does not imply any power-like dependences but a tendency of wave spectra to an asymptotic behaviour controlled mostly by dominating nonlinear transfer. We present this way of analysis as *energy-flux diagram method*.

The key property of the split balance model — *independence of the wave growth on details of wave input function* allows one to use "academic" setup in numerical simulations (Pushkarev, Resio & Zakharov 2003; Badulin et al. 2005) to reproduce the self-similar power-law wave growth (6) in the best way. The "realistic" solutions with conventional input functions (Snyder et al. 1981; Donelan & Pierson-jr. 1987; Plant 1982; Stewart 1974; Hsiao & Shemdin 1983) allow one to quantify the departure from the particular self-similar regimes and to make conclusions on validity of weakly turbulent wave growth laws in general case. The validity check for self-similar solutions consists of two parts. First of all, we check the link of exponents of total energy growth p_τ and of characteristic frequency downshift q_τ (14). This is in line with recent analysis of the fetch-limited growth (Zakharov 2002, Zakharov 2005b).

3.1 Exponents of duration-limited growth. Wave frequency scaling

The split balance model gives a family of solutions (6) that depends on self-similarity index p_τ. To reproduce the solutions for different p_τ "academic" setup can be used (Pushkarev, Resio & Zakharov 2003, Badulin et al. 2005). The idea of this setup is to put wave input in a narrow high-frequency domain $\omega_l < \omega < \omega_h$ to free maximal space for weakly turbulent development of wave spectrum. Total energy grows as follows

$$\frac{\mathrm{d}\varepsilon}{\mathrm{d}t} \sim \int_0^{2\pi} \int_{\omega_l}^{\omega_h} t^{p_{inc}-1} \varepsilon(\omega,\theta) \mathrm{d}\omega\theta \tag{28}$$

where $(p_{inc}-1)$ is exponent of wave energy increment. Note, that exponent p_{inc} is not equal to the resulting exponent of total energy growth p_τ due to dependence of $\varepsilon(\omega,\theta)$ on time. In "realistic" numerical experiments (Snyder et al. 1981, Donelan & Pierson-jr. 1987, Plant 1982, Stewart 1974, Hsiao & Shemdin 1983) increments do not depend on time and the observed exponents p_τ are less than 1.

"Academic" setup allows one to cover a wide range of possible indexes of self-similarity

$$0.191 \le p_\tau \le 1.754; \qquad 0.170 \le q_\tau \le 0.470$$

while the range of "realistic" runs is essentially narrower

$$0.669 \le p_\tau \le 0.835; \qquad 0.243 \le q_\tau \le 0.300$$

(see Table 1). Swell (wave action $N_{tot} = \mathrm{const}$) represents a special case of self-similar solution.

Generally, all the numerical points are slightly above the theoretical straight line (solid line in fig. 2) both for "realistic" and "academic" runs. Moreover, the "realistic" points appear to be very close to the Toba 3/2 law in case of mean frequency scaling (left fig. 2). The departure from the theoretical dependence can be explained easily if we take into account the asymptotic nature of the wave growth

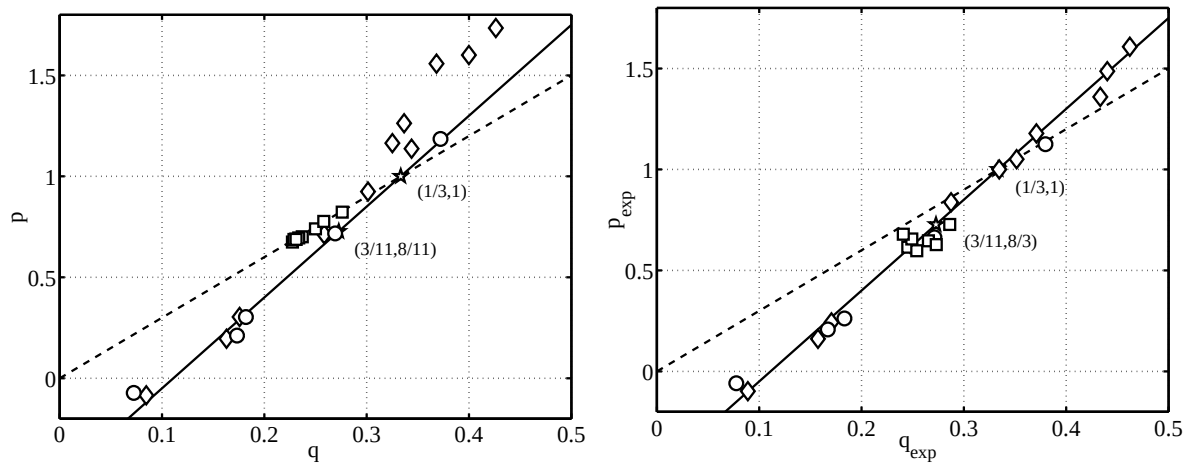

Figure 2: Left — exponents p and q for power-law approximations of total energy and mean frequency of the kinetic equation solutions. Right — exponents p_{exp} and q_{exp} derived from exponents of spectral peak growth α_τ and β_τ (see eq.6,14). ◯ — Isotropic "academic" runs; ◇ — Anisotropic "academic" runs; □ — "Real" wave pumping. Sets of exponents for constant total wave action $(3/11, 8/11)$ and total wave energy $(1/3, 1)$ fluxes are given by stars. Hard line shows theoretical dependence of p_τ on q_τ, dashed line corresponds to Toba's 3/2 law

and the composite nature of the wave spectrum: different parts of wave spectrum attain its self-similar regimes for different times or do not attain these regimes at all due to different composition of wave input and nonlinear transfer. Thus, the resulting wave spectrum is comprised of a self-similar "core" and a non-self-similar "background" (see Badulin et al. 2005, sect. 6.2.3).

Exponents p_τ, q_τ were estimated by two methods. The first method is based on total energy and mean frequency dependencies: the results are shown in left panel fig. 2. An alternative method of estimate of exponents p_τ, q_τ was developed to trace features of the self-similar "core" of the numerical solutions. Exponent q_τ was estimated as $q_\tau = \beta_\tau/2$ (see 14) by tracing the wave action peak frequency and p_τ was found in a similar way from exponent α_τ of wave action magnitude growth (14). The new estimates of p_τ, q_τ collapse to the theoretical dependence remarkably well (right fig. 2).

Strong dispersion of "academic" points relatively to the theoretical line (left fig. 2, especially for $p_\tau > 1$) shows strong effect of non-self-similar background of wave spectra on exponents p_τ, q_τ that cannot be avoided by special setup of numerical experiment: an adequate scaling of wave spectra growth is required to reveal self-similarity features of wave development. The spectral peak characteristics, evidently, fit this requirement better than mean wave frequency. This conclusion is valid for treatment of experimental results: specific methods of measurements can emphasize spectral peak characteristics or, on the contrary, relied on the mean (integral) features. Thus, the observations should be related very carefully to the theoretical predictions.

3.2 Parameter α_{ss} for duration-limited self-similar solutions

Theoretical relationship for total energy and net wave input (27) being rewritten for power-law dependencies

$$\varepsilon = \varepsilon_0 t^p; \qquad \omega = \omega_0 t^{-q}. \tag{29}$$

(all values are dimensional) gives a simple expression for α_{ss}

$$\alpha_{ss}^{(1)} = \left(\frac{\varepsilon_0^2 \omega_0^9}{p_\tau g^4}\right)^{1/3} t^{z_\tau} \tag{30}$$

Run	q_τ	p_τ	z_τ	ε_0	ω_0	$\alpha_{ss}^{(1)}$	$\alpha_{ss}^{(2)}$
ac 7/22	0.170	0.191	-0.049	1.534e-01	4.559	2.245	1.232
ac 5/11	0.181	0.303	-0.008	4.606e-02	5.203	1.283	1.086
ac 8/11	0.254	0.713	-0.047	4.106e-04	12.91	0.633	1.058
ac 19/22	0.289	0.924	-0.082	3.695e-05	19.72	0.416	1.038
ac 1	0.343	1.138	-0.063	3.282e-06	36.73	0.499	0.995
ac 47/44	0.355	1.169	0.048	8.647e-08	82.52	0.487	0.883
ac 25/22	0.366	1.256	0.073	1.164e-08	116.7	0.361	0.841
ac 17/11	0.470	1.754	0.093	1.649e-10	294.2	0.302	0.886
Snyder et al. 10 m/sec	0.247	0.669	0.038	6.740e-04	10.94	0.548	0.843
Snyder et al. 20 m/sec	0.300	0.835	-0.010	1.772e-03	10.84	0.944	0.858
Donelan 10 m/sec	0.243	0.694	0.067	5.848e-04	10.36	0.418	0.841
Hsiao & Shemdin 10 m/sec	0.247	0.685	-0.049	1.694e-04	14.50	0.504	0.878
Hsiao & Shemdin 20 m/sec	0.251	0.699	-0.046	2.303e-03	8.261	0.528	0.863
Hsiao& Shemdin 30 m/sec	0.263	0.734	-0.034	7.799e-03	6.635	0.607	0.855
Stewart 10m/sec	0.281	0.759	-0.004	9.877e-05	19.58	0.838	0.794

Table 1: Exponents and pre-exponents (dimensional) of wind wave growth and self-similarity parameters α_{ss} for numerical runs. Spectral peak frequency was used for scaling the self-similarity law (25). $q^{(1)}$ is calculated as an exponent of power-like approximation (29), $q^{(2)}$ is estimated from the theoretical relation (14). Two different estimates of α_{ss} are given in accordance with formulas (30, 32). Series AC are "academic" for different rates of wave energy growth p_{inc}. Type of wave input parameterization and wind speed are shown for "realistic" cases.

where

$$z_\tau = \frac{2p_\tau - 9q_\tau + 1}{3} \tag{31}$$

and superscript "(1)" for α_{ss} is introduced for the particular case of self-similar solutions (6). Having independent estimates of exponents p_τ, q_τ in numerical runs we, generally, have a dependence of $\alpha_{ss}^{(1)}$ on time. As soon as exponents p_τ and q_τ satisfy theoretical relationship (14) exponent z_τ vanishes and $\alpha_{ss}^{(1)}$ becomes time-independent. Thus, a consistent estimate $\alpha_{ss}^{(1)}$ of self-similarity parameter can be obtained assuming one of exponents of wave growth "more reliable" and using theoretical relation to determine other one. We shall refer to p_τ as a reference one unless otherwise stated. In fact, the departure of exponents from theoretical dependence is relatively small in our case: high power of ω_0 in (30) affects the resulting estimates much stronger.

3.3 Method of energy-flux diagrams

More general expression that does not imply power-law dependence of energy and characteristic frequency on time can be proposed as follows (see 27)

$$\alpha_{ss}^{(2)} = \lim_{t\to\infty} \frac{\varepsilon\omega_*^3}{(g^4 \mathrm{d}\varepsilon/\mathrm{d}t)^{1/3}} \tag{32}$$

Definition (32) looks more attractive and physically transparent as far as it is just a tangent of non-dimensional wave energy and non-dimensional net wave input in the left and right-hand sides of (27).

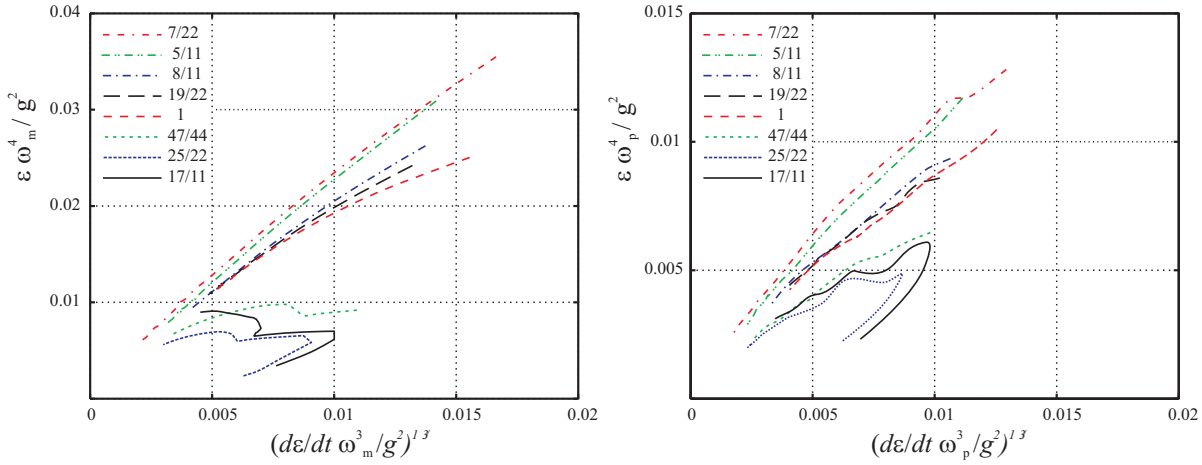

Figure 3: Energy-flux dependences in "academic" experiments for different theoretical exponents of wave growth p_τ (time exponents of wave increments p_{inc} given by eq.28 are shown in legends). Left panel — mean frequency is used for scaling, right panel — peak frequency scales wave energy and wave energy flux. The tendency to self-similarity law is seen much better when peak frequency ω_p is used for scaling. Weak oscillations of trajectories in right panel are due to interpolation from numerical grid. Trajectories are given for $t > 1800$s.

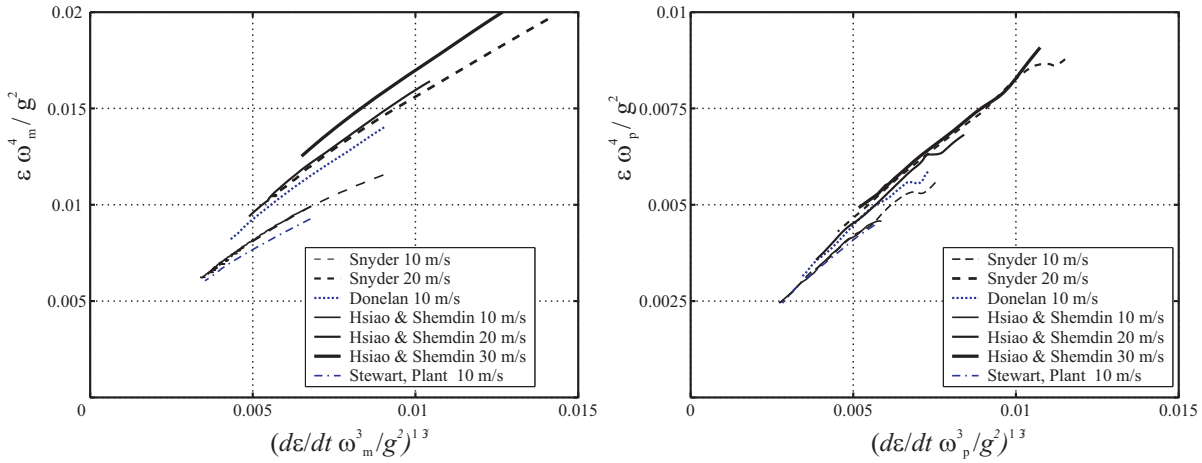

Figure 4: Energy-flux dependences in "real" numerical experiments for different parameterizations of wave input (shown in legends). Left panel — mean frequency is used for scaling, right — peak frequency scales wave energy and wave flux. The tendency to self-similarity law is seen better for stronger winds and wave input functions (Donelan & Pierson-jr. 1987; Snyder et al. 1981). Trajectories are given for $t > 1800$ s.

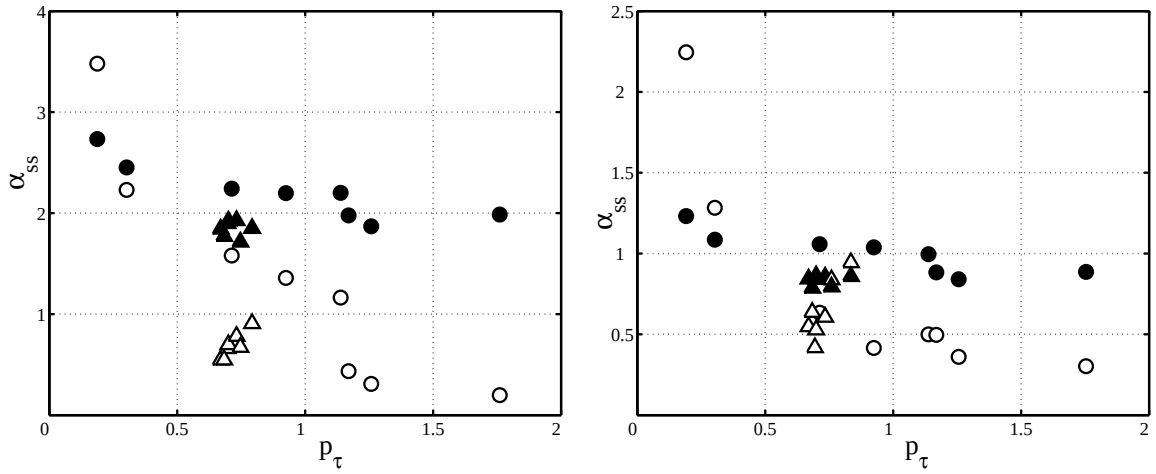

Figure 5: Self-similarity parameter α_{ss} for numerical solutions for duration-limited case. Circles — "academic" wave pumping, triangles — conventional parameterizations of wave input at different wind speeds. Left — mean frequency ω_m is used as a characteristic frequency in (27), right — peak frequency ω_p scaling. Full symbols correspond to estimates (32) and empty ones — to (30).

The existence of the finite limit of $\alpha_{ss}^{(2)}$ can be considered as an independent argument for the validity of the split balance model and, hence, for the dominating role of nonlinear transfer in wave spectra. It is useful to present the corresponding asymptotic analysis in the form of *energy-flux diagrams*.

Fig. 3 shows energy-flux diagram for the set of "academic" numerical runs. Wave input indexes p_{inc} (see 28) are shown in legend. Mean frequency ω_m is used for scaling in left panel while the peak frequency ω_p — in right one. The wave field evolves towards the coordinate origin with time. Trajectories show clear tendency to linear dependence in both panels as it is predicted by the weakly turbulent law (27). For mean frequency scaling (left panel) this tendency is slower and not so pronounced for $p_{inc} > 1$. The peak frequency scaling (right panel) validates the asymptotic law (27) more definitely. An important result of fig. 3 is a weak dependence of the coefficient of proportionality α_{ss} — the self-similarity parameter in (27) on self-similarity index p_τ in very wide range of "academic" setup. It is of great value for practical problems and for cases of realistic wave pumping in numerical runs where the corresponding p_τ varies in narrower range.

Fig. 4 presents the energy-flux diagrams for different conventional parameterizations of wave input (Hsiao & Shemdin 1983, Snyder et al. 1981, Donelan & Pierson-jr. 1987, Stewart 1974) in a range of wind speeds $10 - 30\mathrm{m} \cdot \mathrm{s}^{-1}$. The same tendency to the weakly turbulent energy-flux relationship (27) is seen remarkably well for both frequency scalings (mean frequency — left, peak one — right). As it was expected the asymptotic slope α_{ss} appeared to be very close for all the numerical experiments presented in fig.4 due to relatively low variability of exponent p_τ.

As far as dissimilarity between the "academic" and "realistic" runs is concerned, there is no essential difference in their tendency to the asymptotic behavior. The special academic setup can shorten, in some cases, the time of relaxation to the asymptotic state both due to relatively small non-self-similar fraction of the solutions and due to generally higher (sometimes, intentionally too high) increments of wave growth.

3.4 Self-similarity parameter α_{ss} and pre-exponents of wind-wave growth

Table 1 summarizes results of verification of the self-similarity law (27) for duration-limited case. Downshift exponent q_τ was calculated from time evolution of the spectral peak, linear interpolation was used because of relatively poor frequency grid (71 points in range $0.02 - 2$ Hz) and slowness of downshift itself. Energy exponent p_τ is defined for total energy and, thus, cumulates evolution of self-similar "core"

and non-self-similar background. Exponent z_τ (see 31) represents deviation of p_τ, q_τ from theoretical relationship (14). Pre-exponents ε_0, ω_0 in (29) are given dimensional to avoid the problem of traditional wind speed scaling for "academic" runs. Two last columns present different estimates of self-similarity parameter α_{ss} from (30) and (32). These estimates are presented in fig. 5 for different frequency scalings (left — mean, right — peak frequency).

As it was expected, all the "academic" runs show a gradual trend of α_{ss} with regard to p_τ irrespectively to frequency scaling and definitions (30, 32). "Realistic" cases demonstrate a good conformity with the "academic" reference results. Quality and reliability of the estimates is a subject of special discussion. The definition of α_{ss} as an asymptotic limit (32) looks more consistent. It does not depend on choice of initial moment t_0 and on fitting procedures for approximations (29). The fitting errors due to these, at the first look, unimportant reasons, can affect estimates of (30) dramatically as long as errors in frequency pre-exponent ω_0 in in power 3 (!!!) can lead to essentially higher dispersion of results as compared with "asymptotic" definition (32).

4. EXPERIMENTAL VERIFICATION OF WIND-WAVE GROWTH

Over the years, a great number of field experiments have been undertaken to parameterise behaviour of integral wave properties (wave variance and peak or mean frequency) as the waves develop. Absolute majority of the integral dependences correspond to an ideal stationary case of wave field development in one spatial direction only, while conditions in the perpendicular direction remain homogeneous. Strictly speaking, a relatively small part of these experiments can be related to fetch-limited case: in many of them, the dependence on fetch was simulated by measuring the waves at a single point. Variation of the dimensionless fetch was often achieved by varying the wind speed rather than wave fetch. Therefore, dependences of the wave energy and the peak frequency on the fetch are only as good as the Kitaigorodskii (1962,1983) scaling by the wind speed is correct. Even then, such scaling is bound to bring about a significant scatter both within individual parameterisations and between different experiments (e.g. Kahma & Calkoen, 1992) because the ideal wave development conditions are never met as mentioned earlier in this paper.

Here, we would like to note one positive feature of fetch-limited setup (we mean, obviously, "true" fetch-limited measurements along a number of spatially distributed points) rather than its disadvantages. First of all, such setup has a reference point — a coastline where the wind blows from. It cannot resolve completely the problem of correct account of initial stage of wave development but the problem itself appears to be not so critical as in the duration-limited case: at initial stage waves are relatively short and, hence, slow. Thus, the initial stage for fetch-limited case is relatively short as compared to the duration-limited case. We cannot appreciate the value of this fact in its full extent: numerical study of fetch-limited development has not been done so far and the experimental data are too coarse to identify different stages of wind-wave development.

4.1 Remarks on available data

As we mentioned above the experimental dependencies of wind-wave growth is the only background of our study of fetch-limited case: no numerical results are available up to now to give an alternative verification of self-similarity relationships in the spirit of the above analysis of duration-limited case. Recent analysis by Zakharov (2005) showed that exponents of fetch-limited growth follow remarkably well the self-similarity relationship for 6 fetch-limited experiments. It is not the case for an extensive set of experiments presented in this paper. Moreover, for 50 % of the cases selected by Zakharov (2005) a coincidence rather than a firm agreement takes place: methods of measurements and data analysis could corrupt "true" wave growth dependencies significantly.

At the first glance, the experimental data presented as power-law approximations (27) are "ready-to-use" for verification of the theoretical results. First, the exponents p_χ, q_χ are provided in explicit form and the corresponding theoretical linkage of these exponents

$$p_\chi = \frac{10q_\chi - 1}{2} \tag{33}$$

can be checked trivially in the spirit of Zakharov (2005). Secondly, the total energy flux $\mathrm{d}\varepsilon/\mathrm{d}t$ (the convective derivative) can be calculated analytically. In non-dimensional variables with constant scales of energy, frequency and fetch it gives (compare 30)

$$\alpha_{ss}^{(f)} = \left(\frac{2\tilde{\varepsilon}_0^2 \tilde{\omega}_0^{10}}{p_\chi} \right)^{1/3} \chi^{z_\chi} \tag{34}$$

where

$$z_\chi = \frac{2p_\chi - 10q_\chi + 1}{3} \tag{35}$$

Formula (34) for self-similarity parameter α_{ss} in fetch-limited case looks quite similarly to the duration-limited one (30) and becomes fetch-independent when theoretical relationship for exponents p_χ, q_χ is satisfied, i.e. z_χ in (35) vanishes. It should be stressed that (34) requires scaling by constant value of wind speed U_h in experimental dependencies. The crafty scaling of wave data by instantaneous wind speed or other parameters of air-sea interaction (Davidan 1996) hinders correct weakly turbulent wave physics and makes the corresponding relationships (e.g. 27) useless. Dimensional data are more useful in our case but, generally, unavailable. The scaling can corrupt weakly nonlinear physics in two ways: first, by using instantaneous wind speed scaling, as it was criticized above, secondly, by collecting data from different sources. The latter is often made to have a "more representative" set. Data for different conditions of air-sea interaction (atmosphere stability, gustiness *etc.*) and, hence, for different rates of wave growth being put together are not supposed to satisfy our theoretical relationships.

Wave tank data deserve a special comment. These data are included in a few experimental wave growth dependencies. Strictly speaking such dependencies should be removed from our analysis unconditionally. First, they correspond to very short fetches (a few hundreds wave lengths at the best) and, thus, cannot be related to sea conditions. Secondly, they cannot be related to the kinetic description (within the Hasselmann equation) both because of short time of wave development and because of quasi-unidirectional propagation where essentially two-dimensional four-wave resonances responsible for nonlinear transfer can be suppressed or modified essentially.

4.2 Experimental dependencies of fetch-limited wind-wave grow growth

In this paper we use more than 20 experimental dependences of total wave energy and wave frequency collected in fetch-limited experiments. All the dependences are listed in three groups (see Tables 2, 3) and the groups are given by different symbols in the corresponding figures 6, 7.

The first list (group I in Tables 2, 3) presents the "cleanest" (from the point of view of our theory) results. According to the theory, different conditions of wind-wave development may require different sets of exponents p_χ, q_χ to describe the respective wave growth. Therefore, if the different conditions were initially combined into a single data set, we do not expect results based on such data conform with our theory well. Within the first group, we shall refer to the Black Sea experiment (Efimov, Krivinskii & Soloviev 1986, Babanin & Soloviev 1998) as a reference one, mainly, because the raw data are available for re-analysis. Also, the Black Sea growth dependences agree most closely with the theoretical predictions. All other series of the group are based on measurements at relatively homogeneous conditions of wave growth and measurements in a number of points: the dependence on non-dimensional fetch was not simulated by variation of the wind speed only.

The series of the second list are similar to those of the primary list and demonstrate a reasonably good conformance with the theoretical predictions, but due to data analysis procedures, as outlined in the subsection below, may have suffered some lack of accuracy in terms of their applicability to the theory. Results of this group can be used for our analysis with some caution.

The third list is an antagonist of the first two groups: the collected dependences were obtained for composite data sets, included laboratory data or/and used one-point measurements with further conversion into dependences on dimensionless fetch by varying the wind speed. These data are not expected to conform to our theory and therefore should not be used for comparison and verification of the dependences for the self-similar wave growth.

The dependencies from recent paper by Zakharov (2005) are given in bold in Table 2,3. Note, that only two of these six dependencies fall into the "good lists".

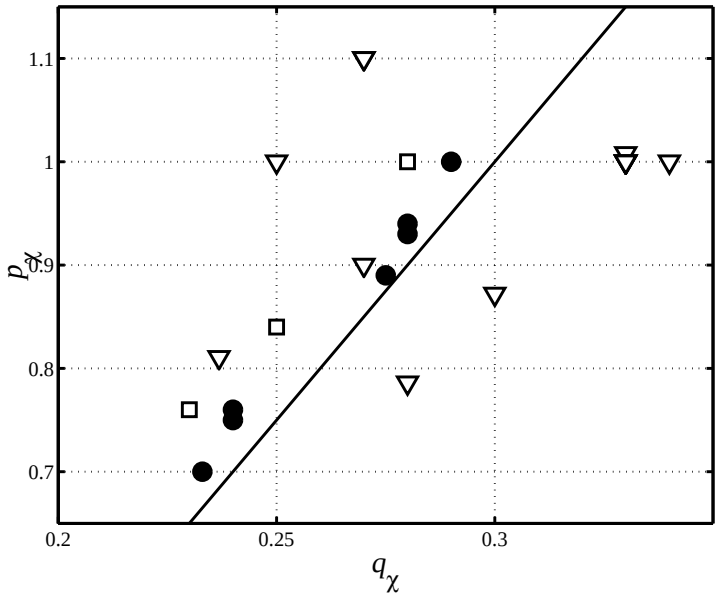

Figure 6: Dependence of p_χ on q_χ for fetch-limited experiments. Dependences from different lists (see Table 2) are given by different symbols: circles — group I, squares — group II, triangles — group III. Solid line — theoretical dependence $p_\chi(q_\chi)$ (33) for fetch-limited growth.

4.3 Exponents of wind-wave growth in fetch-limited experiments

Like in the analysis of duration-limited case, we follow a series of validity checks to show conformance of experimental results to theortical predictions. The results of the first check — exponents of wind-wave growth are presented in Table 2 and in fig. 6 The exponents are given by different symbols for the three groups in order to explain our preferences when creating the separate lists for experimental dependencies.

The first group (1–7 in Table 2) demonstrates the best conformance with the theoretical link of exponents p_χ, q_χ and a slight overestimate of exponent p_χ if compared with its theoretical values. Note, that results of the Black Sea experiment, Dobson et al. (1989), Walsh et al. (1989), Wen et al. (1989), Kahma and Calkoen (1992), Kahma & Pettersson (1994) produce very different p_χ and q_χ exponents being rather close to the theoretical line and, thus, demonstrating a universality of the wave growth dependences in the sense of weakly turbulent law (27) but not in the rigid framework of the "experimental tradition".

Data points of Davidan (1980), Donelan et al. (1985) and SMB CERC (Young 1999) exhibit the same positive bias as well and are in the close proximity to the theoretical relationship, but deviate somewhat further from the line. This positive bias is reproduced in the two lists of the fetch-limited experiments and in the duration-limited numerical runs (see fig. 2) and can possibly be explained by the effect of widening of developing wave spectra (e.g. Babanin & Soloviev 1998, Belberov *et al.* 1983). It is interesting to note, that the regular positive bias is absent in group III of experimental dependencies (see fig. 6). Obviously, for this group fine effects of the spectra widening are buried as a result of inclusion the data which are not consistent with the self-similar development at all.

Reasons for possible deterioration of group II can be suggested. Davidan (1980) used the JONSWAP data set having removed the laboratory data which were employed in the original JONSWAP paper (Hasselmann et al. 1973) to obtain their final dependencies. Scatter of Donelan et al. (1985) data was discussed in detail by Kahma & Calkoen (1992). They argued that this data set could have an additional scatter due to the fact that the stable and unstable stratification data points were used together. Kahma & Calkoen (1992) also pointed out that the Lake Ontario p_χ could have suffered an additional loss of accuracy because Donelan et al. (1985) did not obtain it directly and therefore for their data it is derived from the energy versus peak frequency dependence which is subject to strong spurious correlations. The

	Experiment	$\tilde{\varepsilon}_0 \times 10^7$	p_χ	$\tilde{\omega}_0$	q_χ	z_χ
I	1. Black Sea	4.41	0.89	15.14	0.275	0.010
	2. Dobson et al. (1989)	**12.7**	**0.75**	**10.68**	**0.24**	**0.033**
	3. Walsh (1989) US coast	1.86	1.	14.45	0.29	0.033
	4. Wen et al. (1989)	18.9	0.7	10.4	0.233	0.023
	5. Kahma & Calkoen (1992) unstable	5.4	0.94	14.2	0.28	0.027
	6. Kahma & Calkoen (1992) stable	9.3	0.76	12.	0.24	0.040
	7. Kahma & Pettersson (1994)	5.3	0.93	12.66	0.28	0.020
II	8. Davidan(1980)	4.363	1.	16.02	0.28	0.067
	9. Donelan et al. (1985)	**8.41**	**0.76**	**11.6**	**0.23**	**0.073**
	10. SMB CERC (1977) by Young (1999)	7.82	0.84	10.82	0.25	0.060
III	**11. Mitsuyasu (1971)**	**2.89**	**1.008**	**19.72**	**0.33**	**-0.095**
	12. JONSWAP (1973)	**1.6**	**1.**	**21.99**	**0.33**	**-0.010**
	13. JONSWAP by Phillips (1977)	2.6	1.	11.18	0.25	0.167
	14. Kahma (1981,1986) rapid growth	**3.6**	**1.**	**20**	**0.33**	**-0.100**
	15. Kahma (1986) average growth	2.0	1.0	22	0.33	-0.100
	16. Kahma & Calkoen (1992) composite	5.2	0.9	13.7	0.27	0.033
	17. Evans and Kibblewhite (1990) neutral	2.6	0.872	18.72	0.3	-0.085
	18. Evans and Kibblewhite (1990) stable	5.9	0.786	16.27	0.28	-0.076
	19. Ross (1978) unstable, Michigan	1.2	1.1	11.94	0.27	0.167
	20. Liu & Ross (1980) stratification	0.68	1.1	12.88	0.27	0.167
	21. Donelan et al. (1992) St. Claire	**1.7**	**1.0**	**22.62**	**0.33**	**0.023**
	22. Liu & Ross (1980) corr. Babanin	77	0.52	2.36	0.08	0.413
	23. Hwang & Wang (2004, 2006)	6.19	0.81	11.86	0.237	0.084

Table 2: Exponents and pre-exponents of wind-wave growth in fetch-limited experiments. Cases studied in (Zakharov 2005b) are given in bold

SMB data were obtained in early years of wave research, soon after WWII and are reported here as they are formulated by Young (1999). At those days, measurements and data processing procedures were far less accurate than they are now and even were in the 70s. The SMB CERC curves can be expected to produce some lack of accuracy. In fact, they behave surprisingly well, particularly if compared to those obtained in the 70s and early 80s. Perhaps, one of the possible reasons for such a good conformation with sophisticated dependences of late 80s and 90s is due to the fact that, because of very limiting data recording and processing capacities, the bulk processing was not possible and therefore the data would go through careful selection.

The latter remark is important when considering the third group in Table 2 (nn.11–23). The bulk processing became an option with developing data recording and computer processing facilities and it did not always play a positive role. Kahma & Calkoen (1992) in their thorough investigation of differences between various parameterisations of wave integral properties demonstrated that, for JONSWAP data, many "noisy" spectra were included. In terms of our approach the "noisy" means mixing together occurrences of different growth parameters which leads to an unpredictable average. Once Kahma and Calkoen (1992) performed the separation of different subsets, scatter of the reanalysed data significantly decreased and parameters of the dependencies noticeably changed.

What can cause large deviations, according to our theory, is the use in final JONSWAP dependencies laboratory data. Such data are completely irrelevant to our model of wind-wave sea, the kinetic description of water waves becomes invalid at typical rather short scales of wave development in wave tanks comprising at very best a few hundreds of wave periods. It is interesting to note here that they seemed to have corrupted the peak frequency dependence more than they did the energy dependence. Once Davidan (1980) removed the laboratory data, value of q_χ changed from 0.33 down to 0.28 whereas value of p_χ stayed unchanged.

Thorough analysis of the experimental data is a subject of separate paper. Here we give just a summary of our analysis of the set of dependencies shown in fig. 6. We should say that dependencies nn.1–7 of Table 2 correspond very closely to the predictions of the weak-turbulence theory and therefore were most likely obtained in conditions of self-similar wave development. Dependencies nn.8–10 although exhibit some loss of accuracy, are still very close to the theory and can be used with some caution. The outliers of fig. 6 (nn.11–23) either had non-similar stages embedded or some analysis features imposed which make them unusable for our further analysis.

4.4 Pre-exponents of fetch-limited wind-wave growth

Fig. 7 shows the estimated parameter of self-similarity α_{ss} derived from the experimental dependences discussed above as a function of p_χ in accordance with (34). Thus, based on the experimental dependences, range of "legitimate" changes of the parameter α_{ss} is from 0.3 to 0.65 (or up to 0.75 if the Davidan, 1980 point-at-question is taken into account). We should point out that this range should not be treated as a statistical scatter only around some universal value. Different values of α_{ss} are possible because it is a function of the rate of change of the flux as was mentioned in the previous sections. Variation of α_{ss} for the reference group I is comparable with the duration-limited counterparts for "realistic" numerical runs (see sect. 3.1.3 and Table 1).

These fetch-limited estimates of $\alpha_{ss}^{(f)}$ (eq.34) are slightly below the duration-limited estimates of $\alpha_{ss}^{(2)}$ presented in right fig. 5 and very close to $\alpha_{ss}^{(1)}$ based on similar power-law fit of numerical growth curves (eq. 30). The proximity of duration- and fetch-limited estimates of the self-similarity parameter α_{ss} confirms (may be, somewhat indirectly) the general nature of the weakly turbulent relationship (27): the link of wave energy to the flux (total net input) does not depend on the wave growth setup. In absence of numerical results for the fetch-limited wave development this agreement of the estimates is of special value.

Note, that consistent estimates of α_{ss} in the fetch-limited case look remarkable and can be considered as a recognition of high quality of experimental measurements of wave growth: formula (34) contains the pre-exponent of power fit in high power $\tilde{\omega}_0^{10/3}$ and the pre-exponent $\tilde{\varepsilon}_0$ which varies by more than an order of magnitude for group I. The latter makes estimates of α_{ss} very sensitive to errors of power-law fit. At the same time, all our estimates for "good" groups I and II fall into a fairly narrow range of

	Experiment	p_χ	q_χ^{th}	z_τ	α_{ss}
I	1. Black Sea	0.89	0.278	0.010	0.652
	2. Dobson et al. (1989)	**0.75**	**0.250**	**0.033**	**0.436**
	3. Walsh (1989), US coast	1.0	0.30	0.033	0.302
	4. Wen et al.(1989)	0.7	0.24	0.023	0.533
	5. Kahma & Calkoen (1992) unstable	0.94	0.288	0.027	0.591
	6. Kahma & Calkoen stable	0.76	0.252	0.040	0.520
	7. Kahma and Pettersson (1994)	0.93	0.286	0.02	0.400
II	8. Davidan(1980)	1.0	0.300	0.067	0.751
	9. Donelan et al. 1985	**0.76**	**0.252**	**0.073**	**0.435**
	10. SMB CERC (1977) by Young	0.84	0.268	0.060	0.318
III	**11. Mitsuyasu (1971)**	**1.008**	**0.302**	**-0.095**	**1.138**
	12. JONSWAP (1973)	**1.0**	**0.300**	**-0.100**	**1.106**
	13. JONSWAP by Phillips (1977)	1.0	0.300	0.167	0.160
	14. Kahma (1981,1986) rapid growth	**1.0**	**0.300**	**-0.100**	**1.385**
	15. Kahma (1986) average growth	1.0	0.300	-0.100	1.286
	16. Kahma & Calkoen (1992) composite	0.90	0.280	0.033	0.519
	17. Evans and Kibblewhite (1990), neutral	0.872	0.274	-0.085	0.936
	18. Evans and Kibblewhite (1990), stable	0.786	0.257	-0.076	1.048
	19. Ross (1978), unstable, Michigan	1.1	0.320	0.167	0.116
	20. Liu & Ross (1980), stratification	1.1	0.320	0.167	0.102
	21. Donelan et al. (1992)	**1.0**	**0.30**	**-0.100**	**1.266**
	22. Liu & Ross (1980), corr. Babanin	0.52	0.204	0.413	0.011
	23. Hwang & Wang (2004,2006)	0.81	0.262	0.084	0.373

Table 3: Exponents of wind-wave growth and self-similarity parameter α_{ss} in fetch-limited experiments. q_χ^{th} is calculated from theoretical relation (33) for the observed p_χ, z_τ is detuning exponent in formula for self-similarity parameter α_{ss}. Cases studied in (Zakharov 2005b) are given in bold

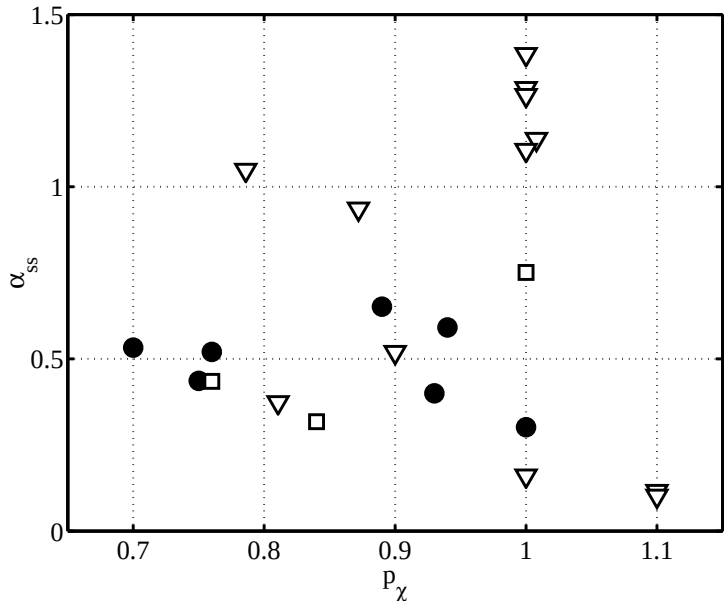

Figure 7: Dependence of α_{ss} on p for fetch-limited experiments.

values.

5. DISCUSSION

5.1 The Toba local balance law of wind-wave growth

Multiple mechanisms and complexity of air-sea interaction nudge researchers to focus on cumbersome models of wind wave growth rather than on compact physics of wind-wave development. The only attempt to construct a concise wave growth law has been undertaken by Toba (1972,1973) in his series of papers in *Journ. Ocean. Soc. Japan.* The 3/2 Toba's law was derived from "the local balance" of weakly nonlinear Stokes drift of water particles and wind stress. The Hasselmann kinetic equation and the associated nonlinear transfer escaped Toba's attention completely. Nevertheless, the conclusions showed a fairly good agreement with observations. Formally, the Toba law can be considered, as a particular case of the weakly turbulent law (27).

Assuming net input $\mathrm{d}\varepsilon/\mathrm{d}t$ be constant one immediately gets the Toba 3/2 law from (27): it corresponds to the stationary energy input through wave development. Let us take the Toba law in the following form (Toba 1997)

$$H_s = B(gu_*)^{1/2} T_s^{3/2}$$

where subscript "s" for period and height means "significant" and $B = 0.062$. Converting significant wave height and wave period into the conventional energy and peak frequency, one has

$$\frac{\varepsilon\omega_p^4}{g^2} = \left(\frac{\pi^9 B^6 u_*^3}{g}\frac{\omega_p^3}{g^2}\right)^{1/3}$$

Comparing with our law (25) one can obtain the rate of total energy accumulated by waves

$$\frac{\mathrm{d}\varepsilon}{\mathrm{d}t} = \frac{\pi^9 B^6 u_*^3}{g} = 0.0017\frac{u_*^3}{g} \tag{36}$$

An evident substitution should be made, taking into account a relative weakness of wind-wave interactions due to differences of air and water densities,

$$\frac{\mathrm{d}\varepsilon}{\mathrm{d}t} = 1.3\frac{\rho_{air}}{\rho_{water}}\frac{u_*^3}{g} \tag{37}$$

The estimate looks reasonable. Significance of the interpretation of the Toba law in terms of the present theory, however, extends far beyond an interesting academic exercise. Since the fetch-limited development commonly exhibits $p_\chi \approx 1$ (see Table 2), i.e. approximately constant energy flux, friction velocity u_* can be used to estimate this flux in such special circumstances according to (37). We must stress here that it is not true in general case: exponents $p_\chi \approx 3/2$ were observed in experiments in Black (Babanin & Soloviev 1998) and Norwegian Seas (Sanders 1976) that corresponds to energy flux growing with time as $\sqrt{t}$.

5.2 Equilibrium range balance of wind-driven waves (Resio, Long & Vincent 2004)

It is important to note that Toba in his study did not refer to the Hasselmann equation and to the corresponding physical mechanisms of nonlinear cascading. In his local balance model he linked nonlinearity of waves (Stokes drift) with wind stress. Within the presented approach we are not able (have no rights, in fact) to relate directly wave growth with characteristics of atmosphere (e.g. u^*). Within the split wave balance we operate with the fluxes of energy (action, momentum) accumulated by the waves, but not with those coming from the wind (i.e. wind input minus dissipation). Thus, in this way, we split, in fact, an inherent dynamics of waves and dynamics of air-sea interaction. A consistent development of our approach, thus, implies a specific "flux language" to fit the wave-wave and air-sea interactions. An important step in this direction has been made recently in (Resio, Long & Vincent 2004).

Authors (Resio, Long & Vincent 2004) related spectral fluxes in the equilibrium range of wind-wave spectra (the frequency range of quasi-constant fluxes) to "an effective, or net, wind input". The proposed parameterization of the net input (eq.19 in Resio, Long & Vincent 2004) is consistent with Toba's estimates (37) and allows one to estimate the total energy from our weakly turbulent law (27)

$$\frac{\varepsilon\omega_p^4}{g^2} = \alpha_{ss}\alpha_4 C_{nl}^{1/3}\frac{u_a - u_0}{C_p} \tag{38}$$

where $C_p = g/\omega_p$ — phase speed of spectral peak waves. In accordance with (Resio, Long & Vincent 2004) $C_{nl} = 0.4$, $\alpha_4 = 0.0053$. Accepting the estimate $\alpha_{ss} = 0.5$ for the self-similarity parameter one has

$$\frac{\varepsilon\omega_p^4}{g^2} = 0.001\frac{u_a - u_0}{C_p} \tag{39}$$

that is very close to the JONSWAP parameterization of wind-wave energy (e.g. Hasselmann et al. 1973, Babanin & Soloviev 1998). Thus, our approach extends results by (Resio, Long & Vincent 2004): the self-similarity and quasi-universality of wind-wave spectra makes valid links of spectra and fluxes in an equilibrium domain for the whole wind-wave range.

6. CONCLUSIONS

We finalize this paper by summarising our results:

i. First of all, the key theoretical result should be emphasized: evolution of growing waves is asymptotically governed by the weakly turbulent law (27,25). This law dictates dependence of the wave energy on spectral flux (total net input). The weakly turbulent law (27) does not depend on such features of wave development as duration- or fetch-limited setup: estimates of the self-similarity parameter α_{ss} from numerical experiments and from experimental dependences for duration- and fetch-limited cases gave remarkably close values;

ii. The theory was verified by means of field experiment data. Available integral fetch-limited dependencies (23 cases) were re-analysed and related to the weakly turbulent self-similar relationships (27,14,33). Those corresponding to the self-similar development were identified on the basis of physics, data quality and initial data processing procedures. We should stress that we did not rely on theoretical results when sorting out the dependencies as "good" or "bad";

iii. The self-similarity parameter α_{ss} should be viewed, if compared with exponents $p_{\tau(\chi)}$, $q_{\tau(\chi)}$, as a more rigid feature of wave development: in spite of difficulties of estimating α_{ss} from experimental and numerical results (e.g. high powers of ω_p in 30,34) it varies in a relatively narrow range which reflects the universality of energy-flux relationship. Experimental estimates of α_{ss} were obtained for the first time. For stable or slowly growing wind speeds we can recommend at the moment $\alpha_{ss} = 0.55 \pm 0.2$: more detailed estimates of this basic physical parameter is a subject of further studies. It was confirmed that fetch-limited and time-limited values of α_{ss} are close which is consistent with the basic concept of weakly turbulent scenario: the concept of rigid link between energy and energy flux.

Other results should be also listed here as important and useful consequences of the general weakly turbulent physics of wind-wave growth.

1. A novel approach to the analysis of wind-wave data — method of energy-flux diagram — was proposed as an effective tool to identify both qualitatively and quantitatively weakly turbulent stage of wind-wave evolution. Its efficiency was illustrated for results of numerical solutions of the Hasselmann equation. Capacity of the method for analysis of a wider set of field experiment data and its consistency with conventional data processing routines should be tested.

2. Analysis of a particular case of constant energy input which corresponds to the Toba 3/2 law shows an important implication of our results for the wind-sea studies: the weakly turbulent relation of energy and flux allows one to determine the net flux coming to waves, based on knowledge of the wave energy. Recent experimental results (Resio, Long & Vincent 2004) gives a remarkable example of consistency of such approach and show its good prospects.

The study refines and essentially extends the concept of universality of wind-wave growth as such: parameters of wave growth are not fixed values for some "ideal" conditions but depend on magnitudes and rates of fluxes of energy (wave action, momentum) to waves and, thus, can be predicted for a much broader range of conditions of growing wind-driven waves.

The research presented in this paper was conducted under the U.S. Army Corps of Engineers, RDT&E program, grant DACA 42-00-C0044, ONR grant N00014-98-1-0070 and NSF grant NDMS0072803, INTAS grant 8014 and Russian Foundation for Basic Research N04-05-64784, ofi-a-05-05-08027 and Russian Academy Program "Mathematical methods of nonlinear dynamics". This support is gratefully acknowledged.

REFERENCES

Abdalla, S. & Cavaleri, L. 2002 Effects of wind variability and variable air density on wave modeling. *J. Geophys. Res.* **107** (C7), doi:10.1029/2000JC000639.

Babanin, A.V. and Soloviev, Yu.P., 1998 Field investigation of transformation of the wind wave frequency spectrum with fetch and the stage of development. *Journ.Phys.Oceanogr.*, **28**, 563–576.

Babanin, A.V. and Soloviev, Yu.P., 1998 Variability of directional spectra of wind-generated waves, studied by means of wave staff arrays. *Mar.Freshwater Res.*, **49**, 89–101.

Badulin S., Pushkarev, A. N., Resio, D. Zakharov, V., 2002 Direct and inverse cascade of energy, momentum and wave action in wind-driven sea. *7th International workshop on wave hindcasting and forecasting*. Banff, October 2002, 92–103.

Badulin S., Pushkarev, A. N., Resio, D. Zakharov, V., 2005 Self-similarity of wind-driven seas. *Nonlinear Processes in Geophysics*. **12**, 891–945.

Belberov, Z.K., Zhurbas, V.M., Zaslavskii, M.,M. & Lobisheva, L.G., 1983 Integral characteristics of wind wave frequency spectra. *Interaction of Atmosphere, Hydrosphere and Lithosphere in Near-Shore Zone of the Sea* (in Russian, English summary), eds: Z.Belberov, V. Zakhariev, O.Kuznetsov., N.Pykhov, B.Filyushkin and M.Zaslavskii. Bulgarian Academy of Science Press, 143–154.

Problems of observations and mathematical modeling of wind waves, 1995 Ed. I. Davidan. St-Peterburg, Meteoizdat, 472 pp. (In Russian).

Davidan I.N., 1980 Investigation of wave probability structure on field data. *Trudi GOIN (in Russian)*, **151**, 8–26.

Davidan I.N., 1996 New results in wind-wave studies, Russian Meteorology and Hydrology, 42–49.

Donelan, M.A., Hamilton, J., Hui, W.H., 1985 Directional spectra of wind-generated waves. *Phil.Trans.R.Soc. Lond.*, **A315**, 509–562.

Donelan, M.A. & Pierson-jr., W.J., 1987 Radar scattering and equilibrium ranges in wind-generated waves with application to scatterometry, *Journ.Geoph.Res.*, **92**, C5, 4971–5029.

Efimov, V.V., Krivinskii, B.B. & Soloviev, Yu.P., 1986 Study of the energetic sea wind waves fetch dependence *Meteorologiya i Gidrologiya*, **11**, 68–75.

Evans, K.C. & Kibblewhite, A.C., 1990 An examination of fetch-limited wave growth off the West coast of New Zealand by a comparison with the JONSWAP results, *J. Phys. Oceanogr.,* **20**, 1278–1296.

Hasselmann, K., 1962 On the nonlinear energy transfer in a gravity wave spectrum. Part 1. *J. Fluid Mech.*, **12**, 481–500.

Hasselmann, K., 1963 On the nonlinear energy transfer in a gravity wave spectrum. Parts 2 and 3. *J. Fluid Mech.*, **15**, 273–281, 385-398.

Hasselmann, K., Barnett, T.P., Bouws, E., Carlson, H., Cartwright, D.E., Enke, K., Ewing, J.A., Gienapp, H., Hasselmann, D.E., Kruseman, P., Meerburg, A., Muller, P., Olbers, D.J., Richter, K., Sell W. & Walden, H., 1973 Measurements of wind-wave growth and swell decay during the Joint North Sea Wave Project (JONSWAP). *Dtsch.Hydrogh.Z.Suppl.*, 12, **A8**.

Hsiao, S.V. & Shemdin, O.H., 1983 Measurements of wind velocity and pressure with a wave follower during MARSEN. *J. Geoph. Res.*, **88**, C14, 9841–9849.

Hwang, P.A. & D. W. Wang, 2004 Field measurements of duration-limited growth of wind-generated ocean surface waves at young stage of development, *J.Phys.Oceanography*, 2316–2326.

Hwang, P.A., 2006 Duration and fetch-limited growth functions of wind-generated waves parameterized with three different scaling wind velocities, *J. Geoph. Res.*, **111**, C02005, doi:10.1029/2005JC003180.

Kahma, K.K., 1981 A study of the growth of the wave spectrum with fetch. *J. Phys. Oceanography*, **11**, 1503–1515.

Kahma, K.K. Calkoen C.J., 1992 Reconciling discreapancies in the observed growth of wind-generated waves. *J. Phys. Oceanography*, **22**, 1389–1405.

Kitaigorodskii, S.A., 1962 Applications of the theory of similarity to the analysis of wind-generated wave motion as a stochastic process, *Bull.Acad.Sci. USSR, Geophys. Ser., Engl. Transl.*, **N1**, 105–117.

Kitaigorodskii, S.A., 1983 On the theory of the equilibrium range in the spectrum of wind-generated gravity waves, *Journ.Phys.Oceanography,* **13**, 816–827.

Liu P.C. & D.B. Ross, 1980 Aiborne measurements of wave growth for stable and unstable atmospheres in Lake Michigan, *J. Phys. Oceanogr.,* **10**, 1842–1853.

Mitsuyasu, H., Nakamura, R. & Komori, T., 1971 Observations of the wind and waves in Hakata Bay, *Report of the Research Institute for Applied Mechanics, Kyushu University,* **19**, 37–74.

Plant W.J., 1982 A relationship between wind stress and wave slope. *Journ.Geoph.Res.*, **87**, C3, 1961–1967.

Pushkarev, A.N., Resio, D. & Zakharov, V.E., 2003 Weak turbulent theory of the wind-generated gravity sea waves. *Physica D: Nonlinear Phenomena*, 184, 29–63.

Pushkarev, A.N., Resio, D. & Zakharov, V.E., 2004 Second generation diffusion model of interacting gravity waves on the surface of deep water, *Nonlin. Processes Geophys.*, **11**, 329–342.

Resio D.T., Long C.E., Vincent, C.L, 2004 Equilibrium-range constant in wind-generated wave spectra, *Journ.Geophys.Res.,* **109**, C01018, doi:1029/2003JC001788.

Sanders, J. W., 1976 A growth-stage scaling model for the wind-driven sea, *Ocean Dynamics*, **29**, 136–161.

Snyder, R.L., Dobson, F.W., Elliot, J.A. and Long, R.B., 1981 Array measurements of atmospheric pressure fluctuations above surface gravity waves, *J. Fluid. Mech.*, **102**, 1–59.

Stewart, R.W., 1974 The air-sea momentum exchange, *Boundary-Layer Meteorology*, **6**, 151–167.

Toba, Y., 1972 Local balance in the air-sea boundary processes I. On the growth process of wind waves, *J. Oceanogr.Soc.Japan*, **28**, 109–121.

Toba, Y., 1972 Local Balance in the Air-Sea Boundary Processes II. Partition of Wind Stress to Waves and Current, *J. Oceanogr.Soc.Japan*, **29**, 70–75.

Toba, Y., 1973 Local balance in the air-sea boundary processes. III. On the spectrum of wind waves, *J. Oceanogr.Soc.Japan*, **29**, 209–220.

Toba, Y., 1997 Wind-wave strong wave interactions and quasi-local equilibrium between wind and wind sea with the friction velocity proportionality, In: *Nonlinear ocean waves. Advances in Fluid Mechanics*. Ed. W.Perrie, **17**, 1–59.

Shore Protection Manual, 1977 Corps of Engineers. USA-CERC (U.S. Army Coastal Engineering Research Center). Ed. USACERC. Department of the Navy. 3rd Fort Belvoir, Virginia. USA. **1–3**.

Walsh E.J, Hancock III D.W., Hines D.E., 1989 An observation of the directional wave spectrum evolution from shoreline to fully developed. *J. Phys. Oceanogr.*, **19**, 670–690.

Wen S.C., Zhang D., Peifang G. & Bohai, C., 1989 Parameters in wind-wave frequency spectra and their bearings on spectrum forms and growth, *Acta Oceanologica Sinica*, **8**, 15–39.

Young, I.R., 1999 Wind Generated Ocean Waves, Elsevier.

Zakharov, V.E., 1966 Problems of the theory of nonlinear surface waves, PhD thesis, Budker Institute for Nuclear Physics, Novosibirsk, USSR.

Zakharov, V.E. & Filonenko, N.N., 1966 Energy spectrum for stochastic oscillations of the surface of a fluid, *Dokl.Acad.Nauk SSSR*, **160**, 1292–1295.

Zakharov, V.E., 1992 Direct and inverse cascade in wind-driven sea and wave breaking Proceedings of IUTAM Meeting on Wave Breaking (Sydney, 1991), eds. M.L. Banner and R.H.Y. Grimshaw. Springer-Verlag, Berlin, 69–91.

Zakharov, V.E., 1999 Statistical theory of gravity and capillary waves on the surface of a finite-depth fluid *Eur.J.Mech. B/Fluids*, **18**, 327–344.

Zakharov, V.E., 2002 Theoretical interpretation of fetch limited wind-driven sea observations. 7th International workshop on wave hindcasting and forecasting, Banff, October 2002, 86–92.

Zakharov, V.E., 2005 Direct and inverse cascades in the wind-driven sea. AGU Geophysical Monograph, Miami, 1–9.

Zakharov, V.E., 2005 Theoretical interpretation of fetch limited wind-driven sea observations. *Nonlin. Proc. Geophys.*, **12**, 1011–1020.

Zakharov, V.E. & Zaslavsky, M.M. 1982 The kinetic equation and Kolmogorov spectra in the weak-turbulence theory of wind waves, *Izv.Atm.Ocean.Phys.*, **18**, 747–753.

Zakharov V.E., L'vov, V.S. & Falkovich, G.C., 1992 Kolmogorov Spectra of Turbulence. I. Wave Turbulence, Series in nonlinear dynamics, Springer–Verlag.

Zakharov, V.E. & Pushkarev, A.N., 1999 Diffusion model of interacting gravity waves on the surface of deep fluid, *Nonlin.Proc. in Geophysics,* **6**, 1–10.